Cationic Photopolymerization of Biobased Oxetane Monomers Obtained from Adipic, Itaconic, and Citric Acid Functionalization

Macromolecular Chemistry and Physics

Macromolecular Chemistry and Physics
www.mcp-journal.de

RESEARCH ARTICLE OPEN ACCESS

Cationic Photopolymerization of Biobased Oxetane Monomers Obtained from Adipic, Itaconic, and Citric Acid Functionalization

Dumitru Moraru[1] | Lazaros Papadopoulos[2] | Minna Hakkarainen[2] | Marco Sangermano[1]

[1]Department of Applied Science and Technology, Politecnico di Torino, Torino, Italy | [2]Department of Fibre and Polymer Technology, KTH Royal Institute of Technology, Stockholm, Sweden

Correspondence: Marco Sangermano (marco.sangermano@polito.it)

Received: 19 May 2025 | **Revised:** 15 July 2025 | **Accepted:** 29 July 2025

Funding: This paper is part of a project that received funding from the European Union's Horizon 2020 research and innovation program under the Marie Skłodowska-Curie grant agreement, No 101085759 (SURE-Poly). This manuscript reflects only the authors' views and opinions; neither the European Union nor the European Commission can be considered responsible for them.

Keywords: adipic acid | bio-based | cationic photopolymerization | citric acid | itaconic acid | oxetane | UV-curing

ABSTRACT

Cationic photopolymerization offers a significant advantage over radical polymerization due to its resistance to oxygen inhibition and superior dimensional stability during the crosslinking process. In this study, we aim to advance the development of bio-based monomers for cationic photopolymerization by synthesizing oxetane-functionalized derivatives of adipic, itaconic, and citric acids. These three renewable acids were chosen for their multifunctionality and availability. The synthesized monomers, bis((3-methyloxetan-3-yl)methyl) adipate (BOA), bis((3-methyloxetane-3-yl)methyl) itaconate (BOI), and tris((3-methyloxetane-3-yl)methyl) citrate (TOC), were fully characterized using nuclear magnetic resonance (NMR). Fourier transform infrared (FTIR) spectroscopy and photo differential scanning calorimetry (photo-DSC) were employed to monitor the oxetane ring-opening reaction kinetics and to determine the degree of conversion, revealing high reactivity in all monomers, reaching nearly complete conversion within 90 s. The mechanical properties of the UV-cured films were assessed by dynamic mechanical thermal analysis (DMTA) and gel content measurements. Results indicated that the BOI-based films exhibited higher glass transition temperatures (Tg) and crosslinking densities compared to BOA- and TOC-based films. The findings demonstrate the potential of bio-based oxetane monomers to produce UV-curable materials with acceptable thermomechanical properties, offering a sustainable alternative to petroleum-derived precursors.

1 | Introduction

In a more sustainable and forward-thinking global framework, the research on biobased monomers plays a crucial role in replacing fossil-based alternatives [1–10]. Biomass feedstock, an abundant carbon source, can be transformed into various value-added chemicals and serves as a promising renewable alternative to fossil fuels [11–13]. Shifting focus to the technology, UV-curing is an efficient and sustainable method for producing solid materials from liquid monomer formulations. This technique has found applications in industries such as coatings, dental products, and additive manufacturing, offering key advantages, including the absence of volatile organic compound (VOC) emissions due to the lack of solvents and reduced energy consumption [14].

Among the various monomer crosslinking strategies, cationic ring-opening photopolymerization is a UV-curing process that offers significant advantages over radical polymerization, as it is unaffected by oxygen inhibition and promotes dimensional stability during the crosslinking process [15, 16]. Epoxy resins are the most used monomers in cationic polymerization, widely applied in coatings, inks, nanocomposites, and adhesives [17–19]. These monomers exhibit high reactivity due to the heteroatom in the epoxy ring, which is highly susceptible to protonation during cationic ring-opening polymerization. This reactivity is attributed to the significant ring strain and the electronegativity of the heteroatom [20, 21].

Three decades ago, monomers bearing oxetane functionalities emerged as another interesting option for cationic polymerization [22–24]. The oxetane ring is a four-membered cyclic ether that, like the epoxide (oxirane) ring, experiences significant ring strain, with values comparable to ethylene oxide (107 $kJmol^{-1}$ for oxetane and 114 $kJmol^{-1}$ for oxirane). However, the oxygen atom in the oxetane ring exhibits greater basicity than that in oxirane, as indicated by their pKa values (2 for oxetane and 3.7 for oxirane) [25, 26]. Since then, only a limited number of studies have been published on the cationic photopolymerization of oxetane-functionalized monomers, with none, to our knowledge, focusing on bio-based systems. As a contribution from our group, in previous studies, we have investigated in depth the reactivity of oxetane monomers toward solvent-free cationic photopolymerization and the properties of crosslinked films [27–29]. In 2016, Zheng et al. investigated the copolymerization of oxetane with epoxy monomers to enhance the reactivity and final oxirane conversion [30]. However, in recent years, research on oxetane monomers appears to be stagnant. In a more eco-sustainable approach, we would like to reboot the use of oxetane monomer in cationic photopolymerization utilizing renewable precursors. To this end, we employed three biobased monomers that are widely available, namely adipic acid, itaconic acid, and citric acid.

Adipic acid is a dicarboxylic acid and can be produced from biomass mainly via chemocatalytic and biological methods. It is extensively used in the production of polyamides, polyurethane resins, adhesives, and lubricants among other products [31–34].

Itaconic acid is an unsaturated dicarboxylic acid, which is produced via fermentation of carbohydrates by fungi, with a market volume of thousands of tons per year [35], and several reviews on the exploitation of itaconic acid as a bio-based precursor have been published [36–39].

Citric acid is a tricarboxylic acid, which is a common metabolite of plants present in the juice of citrus fruits and can also be easily obtained as a fermentation product from carbohydrate metabolism of many aerobic and anaerobic microorganisms [40].

All these acids are multifunctional and would serve as ideal precursors to prepare monomers with oxetane moieties for cationic photopolymerization. Thereby, the three biobased acids were functionalized with 3-ethyl-3-oxetane methanol, via one pot transesterification reaction, to achieve bio-based photocurable oxetane monomers (see Scheme 1).

The synthesized bis((3-methyloxetan-3-yl)methyl) adipate (BOA), bis((3-methyloxetane-3-yl)methyl) itaconate (BOI), and tis((3-methyolxetane-3-yl)methyl) citrate (TOC) were fully characterized by NMR analysis and investigated in cationic UV-curing relativity. The curing process was followed by FTIR and photo-DSC analysis, and the thermo-mechanical properties of the crosslinked network were investigated by DSC and DMTA analysis.

2 | Discussion

2.1 | Synthesis of Oxetane Monomers

The monomers of this study were prepared via a conventional transesterification reaction (see Scheme 1). Preliminary experiments were used to determine the temperature and the amount of catalyst for the preparation of each monomer. Reaction temperatures higher than 170°C resulted in gelation of the reaction mixture, while a higher amount of catalyst was used for the preparation of TOC monomer, as the larger, more branched structure, including three carboxyl groups and an additional hydroxyl group of TEC increased the viscosity of the mixture significantly, limiting the yield of the reaction.

BOA was received as a transparent liquid of relatively low viscosity, while BOI and TOC were of yellow to orange colour and their viscosity was higher, potentially due to the C═C bond and the free ─OH group in their structure, respectively. The yield of the transesterification reaction was calculated by comparing the ratio of the signals of the esters of the precursors (DMA, DMI, TEC) with the signals of the OxMe esters of the prepared monomers. For DMA and DMI precursors, a conversion of methyl esters above 95% was achieved. In the case of the TEC precursor, the increased viscosity limited the conversion of the ethyl esters. While the spectrum is more complex compared to the rest of the monomers, a conversion between 85 and 90% is expected.

The synthesized monomers were fully characterized by ^{1}H-NMR and ^{13}C-NMR analysis. The detailed assignments are reported in the experimental part.

2.2 | Photo-Curing Kinetics

Figure 1 shows the spectra of the BOI monomer under UV-light, recorded at 25°C, with magnifications centred at 1648 cm^{-1} (A) and 835 cm^{-1} (B), as an example. The oxetane conversion was calculated using Equation (1), and conversion curves as a function of irradiation time are reported in Figure 2 for the investigated monomers. The ring-opening reaction was strongly influenced by the temperature at which the crosslinking process is carried out, as previously reported by Crivello et al. [24, 25, 41]. For this reason, we have investigated, as a first step, the influence of temperature during cationic photopolymerization of synthesized oxetanes. The studied monomers showed relatively high reactivity of the oxetane group when the photo-curing process was conducted at temperatures of 85°C and above.

The BOA-based formulation showed a very sluggish reactivity at 25°C, as Figure 2 illustrates, reaching 63% conversion upon 90 s

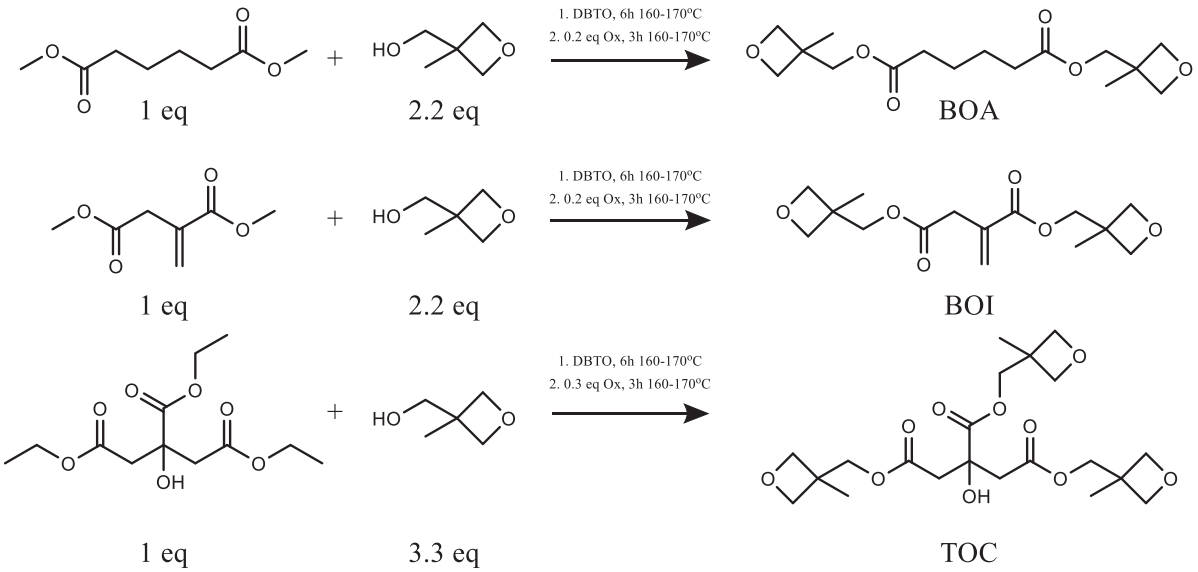

SCHEME 1 | Synthetic route for the oxetanes synthesis.

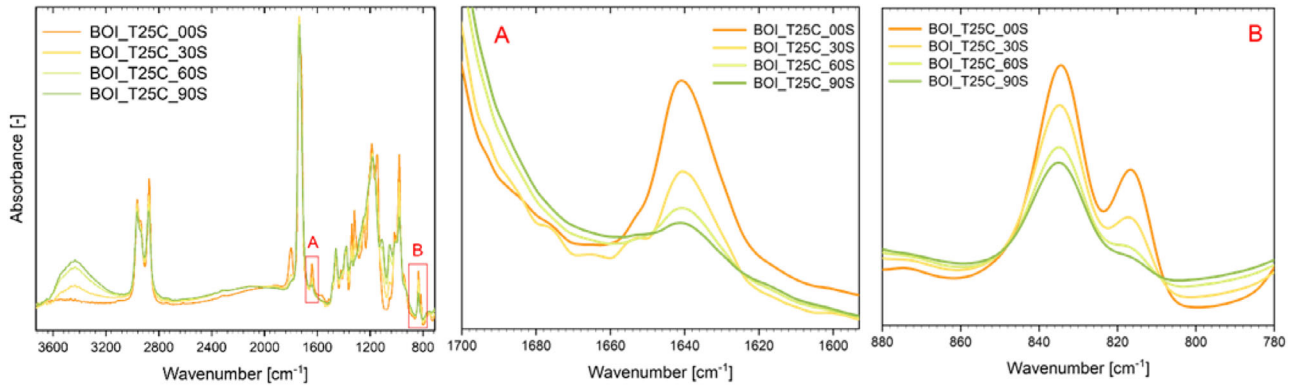

FIGURE 1 | RT-FTIR spectra of BOI formulation; the decreasing of the vinyl group at 1648 cm^{-1} (A) and the oxetane group at 835 cm^{-1} and the C═C group at 816 cm^{-1} (B).

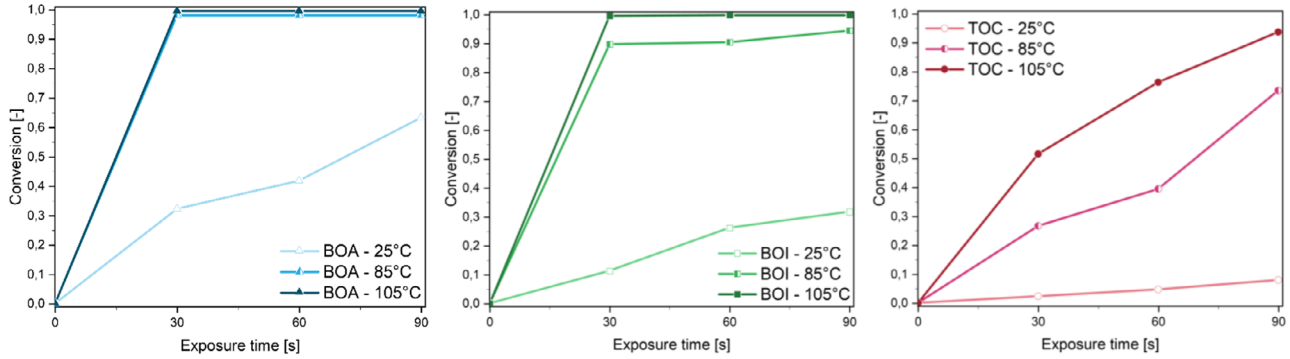

FIGURE 2 | Conversion curves for oxetane groups as a function of irradiation time of BOA, BOI, and TOC monomer (signal monitoring at 835 cm^{-1}).

of UV-irradiation. By raising the temperature to 85°C and 105°C, an enhancement in the curing kinetics can be observed and most of the oxetane groups react within just 30 s to almost complete conversion (98% and 99% respectively).

The BOI monomer showed, as well, low reactivity at room temperature, with a conversion of the oxetane group of 32%. However, this formulation also reacted rapidly once sufficient thermal energy was provided, as the conversion reached 94%

after 90 s of irradiation at 85°C and reached close to complete conversion (99%) at 105°C.

It is important to underline that thicker samples of BOA-based formulations were not fully crosslinked, while formulations based on BOI monomer reached an adequate crosslinking degree even in the case of thicker samples at room temperature (samples of 500 μm thickness for DMTA analysis). Following the FTIR spectra upon irradiation, it is possible to observe a decrease in the C═C double bond peak, both measured at 1648 and at 816 cm^{-1}, along with the reduction of the oxetane group peak at 835 cm^{-1} (Figure 1A,B). This suggests that the C═C double bonds are involved in the curing reaction. This was unexpected, and we suppose it could be due to the radical formed during onium salt photodecomposition. It seems that the C═C bond shows quite good reactivity toward radical chain-growth polymerization promoted by the radical byproduct obtained during irradiation. This could also be the reason why the irradiated BOI formulations resulted in crosslinked films even when the process was conducted at 25°C. We assume that BOI monomer acts as a trifunctional monomer, involving 2 oxetane functionalities and a C═C double bond functionality, all involved in the polymer network formation.

The conversion curves clearly show that the trifunctional oxetane (TOC) exhibits the slowest reaction kinetics among the three monomers. At room temperature, the ring-opening reaction progresses slowly, achieving only 8% conversion after 90 s of UV irradiation at 25°C. When the curing process is performed at 85°C, an oxetane group conversion of 73% was achieved. Then again, when curing was performed at 105°C, an overall conversion of 90% was reached within the same time. The slightly lower reactivity of the trifunctional monomer was expected. Normally, during the curing of a trifunctional monomer, a vitrification effect should occur faster compared to a bifunctional one, leading to a decrease of the polymer chain mobility and eventually to a stop of the chain growth.

A gel content exceeding 98% in BOI- and TOC-based materials confirmed the formation of a fully crosslinked network, whereas the BOA-based material exhibited a gel content of 89%.

Photo-DSC analysis was conducted at various temperatures to evaluate the heat release during the crosslinking reaction. As shown in Figure 3, the BOI-based formulation exhibited the highest heat release across all temperatures studied. The BOA-based formulation showed comparable heat release at 120°C, despite FTIR results indicating good reactivity at 85°C as well. In contrast, the TOC-based formulation displayed lower reactivity among the three studied monomers, aligning with the observations from FTIR analysis.

These differences can be attributed to both chemical and physical factors. The higher enthalpy of BOI compared to BOA is due to the presence of a carbon-carbon double bond in its structure, enabling concurrent radical and cationic photopolymerization. FTIR data confirm this dual mechanism, and the additional radical curing contributes to the total heat measured in Photo-DSC. Despite its trifunctionality, TOC's lower heat release is likely due to the high viscosity of the monomer and early gelation, the latter being a consequence of its higher functionality, which

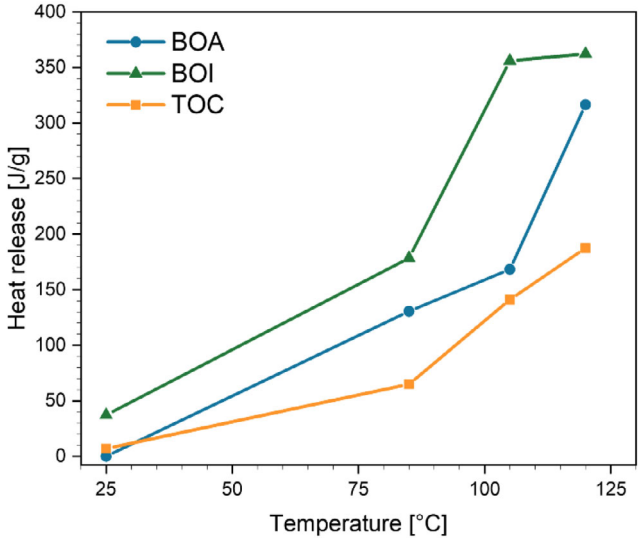

FIGURE 3 | Heat release during the crosslinking reaction of all three monomers, BOA, BOI, and TOC at different temperatures (25°C, 85°C, 105°C, and 120°C).

TABLE 1 | FTIR Conversions and photo-DSC heat releases for BOA, BOI, and TOC formulations.

Curing Temperature		FTIR 90s Conversion	Photo-DSC Heat release (J/g)
BOA	25°C	63%	0
	85°C	98%	131
	105°C	100%	168
BOI	25°C	32%	37
	85°C	95%	179
	105°C	100%	356
TOC	25°C	8%	7
	85°C	74%	65
	105°C	94%	141

together limit oxetane conversion. Rapid network formation restricts chain mobility, reducing the extent of the reaction. In contrast, the bifunctional formulations of BOA and BOI exhibit slower network buildup, allowing mobility and more complete conversion before gelation. Furthermore, it is also important to consider differences in experimental setup: FTIR measurements were performed on 12 μm films, whereas Photo-DSC used approximately 7 mg of bulk material in an aluminium pan, potentially influencing the observed reactivity and heat release (Table 1).

2.3 | Characterization of Thermo-Mechanical Properties of UV-Cured Films

Viscoelastic properties of the UV-cured formulations were evaluated by DMTA analysis (curves reported in Figure 4). The crosslinked density was assessed following Equation (2), consid-

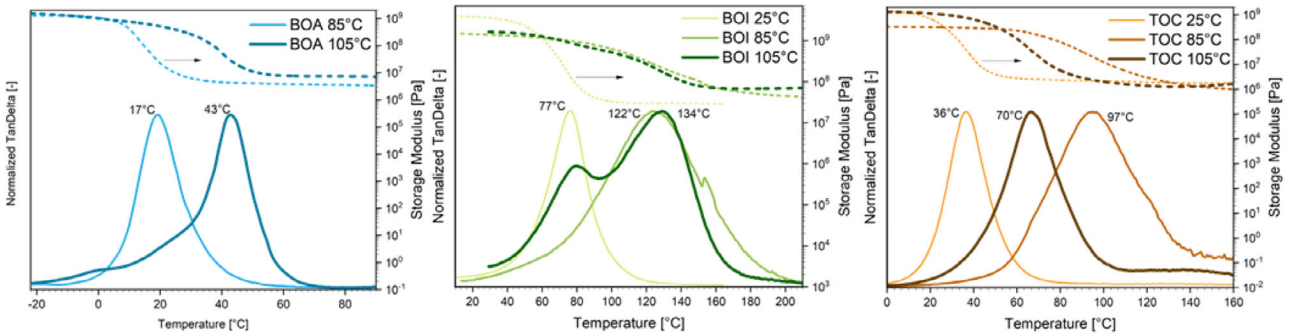

FIGURE 4 | DMTA curves of UV-Cured films of BOA, BOI, and TOC.

ering the modulus value measured at Tg + 50°C, from the storage modulus curves E'.

The thermo-mechanical properties of the cured films, evaluated by DMTA, exhibit a strong dependence on the curing temperature and the structural features of the monomers. For the BOA-based system, no crosslinked film could be obtained under UV irradiation at room temperature, indicating very limited oxetane reactivity under these conditions. Upon increasing the curing temperature, fully crosslinked materials were obtained, and the glass transition temperature (Tg) increased from 17°C (when curing at 85°C) to 43°C (when curing at 105°C), in agreement with the progressive increase in oxetane conversion and crosslinking density observed in FTIR and Photo-DSC analyses.

The BOI-based formulation exhibited significantly higher Tg values compared to BOA across all curing conditions. The sample exhibited a Tg of 77°C after curing at 25°C. When cured at 85°C, the DMTA curve displayed two distinct transitions, at 80°C and 122°C, suggesting the formation of a heterogeneous network with regions of different crosslinking density. This is consistent with FTIR results showing that at room temperature, the radical polymerization of C═C groups dominates with limited oxetane conversion (32%). When the crosslinking reaction occurred at 85°C, activation of oxetane rings occurs, but incomplete conversion may lead to structural heterogeneity, as suggested by the presence of multiple transitions. At 105°C, full activation of both functional groups is achieved, yielding a more homogeneous and highly crosslinked network, as evidenced by the single Tg peak at 134°C and the highest enthalpy release observed in Photo-DSC. The superior performance of BOI can be attributed to its bifunctional structure, which enables both radical polymerization of the C═C double bonds and cationic ring-opening polymerization of the oxetane, contributing to increased crosslinking density and network stiffness. Additionally, the higher flexibility of the adipate backbone in BOA compared to the more rigid itaconate unit in BOI contributes to the differences in network stiffness and final Tg.

In contrast, TOC-based systems exhibited a decrease in Tg when cured at 105°C (70°C) compared to 85°C (97°C), despite their trifunctional design. This counterintuitive behaviour may result from two competing effects. First, the high functionality leads to rapid network formation and early gelation, which restricts oxetane conversion and limits overall crosslinking density. Second, the presence of hydroxyl groups in the TOC structure can promote chain transfer reactions via the activated monomer mechanism, forming flexible ether linkages that reduce network rigidity. It is well known that OH groups could interact with the carbocationic growing chain via a chain transfer reaction, enhancing the ring-opening conversion [42–44]. In the presence of hydroxyl groups, the growing chain is terminated by reaction with the OH, an ether linkage is formed, and simultaneously, a proton is produced, which can initiate a new polymeric chain. Moreover, it is likely enhanced at higher temperatures, which could explain the observed drop in Tg at 105°C curing temperature. These factors are reflected in the lower νc values and reduced modulus observed for TOC-based materials. The BOI system, on the other hand, benefiting from both radical and cationic reactivity, clearly outperforms the other formulations in terms of crosslinking density and thermal resistance. The summarized data are presented in Table 2.

Contact angle on UV-Cured films were measured with bi-distilled water (values reported in Table 2. Images reported in Figure 5), the TOC film exhibits a contact angle value of around 92°, which is definitely a higher hydrophobicity than the BOI film, exhibiting a contact angle of around 72°.

3 | Conclusion

To awaken the research interest in the exploitation of oxetane monomer in cationic photopolymerization, we have selected three bio-based precursors: adipic, itaconic, and citric acid, which were functionalized with oxetane ring functional groups. The synthesis of the oxetane monomers was achieved via a conventional transesterification reaction, starting from the esters of the acid functionalized with 3-ethyl-3-oxetane methanol. The synthesized monomers were fully characterized by NMR analysis, and their reactivity toward cationic photopolymerization was investigated via FTIR and photo-DSC.

The conversion curves as a function of irradiation time showed a good reactivity of the monomers with an almost complete oxetane group conversion for all monomers when the curing process was performed at 85°C or above. Compared to oxetane BOA, a slightly better reactivity was evidenced for BOI, which seems to behave as a trifunctional monomer involving the curing process the C═C double bond besides the oxe-

TABLE 2 | Thermo-mechanical properties measured by DMTA analysis of UV-Cured oxetane films.

Curing Temperature		DMTA Tg (°C)[1]	Modulus (Pa)[2]	νc (mmol/cm^3)[3]	Contact angle (°)[4]	Gel content (%)
BOA	25°C	N/A	N/A	N/A	NA	NA
	85°C	17	3.69×10^6	0.43	93 ± 4	89
	105°C	43	7.03×10^6	0.77	95 ± 6	89
BOI	25°C	77	2.99×10^7	3.00	NA	NA
	85°C	80/122	5.68×10^7	5.09	72 ± 4	100
	105°C	134	7.10×10^7	6.29	73 ± 5	100
TOC	25°C	36	1.47×10^6	0.16	NA	NA
	85°C	97	1.24×10^6	0.12	92 ± 3	100
	105°C	70	1.41×10^6	0.14	94 ± 2	100

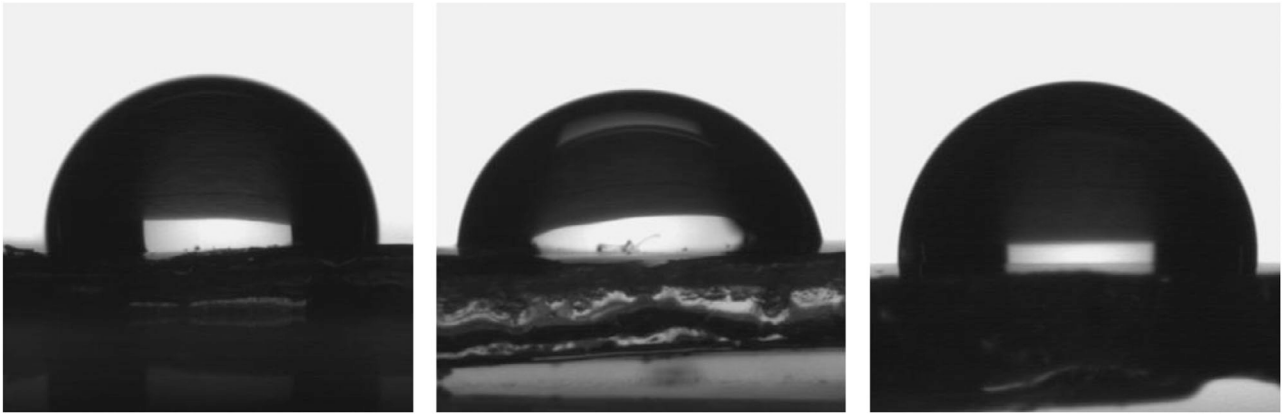

FIGURE 5 | Contact angle on UV-cured films of BOA (left), BOI (center), and TOC (right) crosslinked at 85°C.

tane ring. The TOC behaviour was explained mainly because of the activated monomer mechanism involving OH groups, which causes a reduction of the crosslinking density and formation of ether flexible linkages in the polymeric structure. In fact, during the polymerization reaction, the growing ionic chain end undergoes nucleophilic attack by the hydroxyl group present in the TOC monomer to give a protonated ether. Deprotonation of this latter species by the oxetane monomer results in the termination of the growing chain and the proton transfer to a new oxetane monomer, which can start a new chain. The resulting polymers have flexible ether linkages and a lower Tg. This mechanism is responsible at the same time of the good oxetane group conversion but lower crosslinking density of TOC crosslinked monomer with respect to BOI.

The UV-cured materials were characterized by DMTA analysis, and the crosslinked bifunctional oxetane BOI showed a higher Tg value compared to the other crosslinked monomers due to the smaller structure and additional functionality provided by the double bond, leading to higher crosslink density.

We have shown the possibility to widen the availability of bio-based cationic UV-curable monomers, prone to the photocuring process, giving rise to UV-cured films with good thermo-mechanical properties and tunable Tg.

4 | Experimental Section

4.1 | Materials

Dibutyl tin oxide (DBTO, 98%), 3-methyl-3-oxetane methanol (OxMe, 98%), adipic acid dimethyl ester (DMA, ≥99%), itaconate dimethyl ester (DMI, 97%), citrate triethyl ester (TEC, 98%), triarylsulfonium hexafluoroantimonate salts (50% of solids by weight in propylene carbonate) and chloroform were all purchased from Aldrich. (Sigma–Aldrich AB, Stockholm, Sweden).

4.2 | Oxetane Monomer Synthesis

In a round-bottom flask, DMA, DMI, or TEC and OxMe, in an excess of 0.1 eq per ester functional group, and DBTO were added. The flask was purged with nitrogen, and the temperature was increased gradually to 160°C. The reaction mixture was stirred vigorously with a magnetic stirrer and was kept at 160°C for 3 h and at 170°C for another 3 h. The mixture was then cooled down to room temperature, and a second part of 3-methyl-3-oxetane methanol was added, equal to 0.1 eq per ester functional group. The mixture was then reheated at 160°C for 1.5 h and at 170°C for another 1.5 h. The temperature was then set at 140°C, and a vacuum of 5 mbar was applied for 3 h, to remove unreacted OxMe. Then the apparatus was cooled down to room

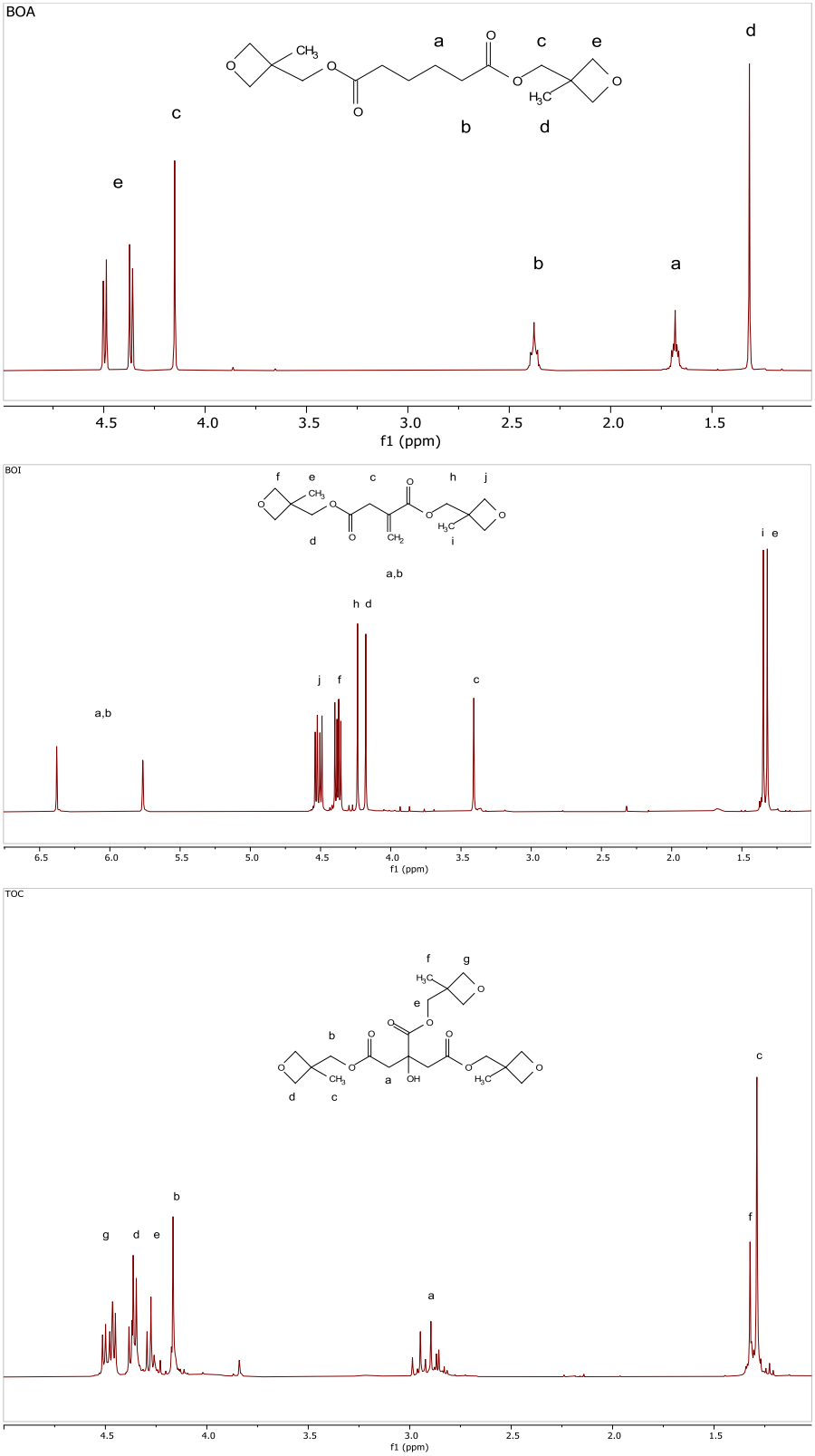

FIGURE 6 | ^{1}H-NMR analysis of the synthesized oxetane monomers; BOA, BOI, TOC.

temperature to collect the monomers. No purification was made prior to characterization. The scheme of the synthetic procedure is reported in Scheme 1.

The synthesized monomers were fully characterized by ^{1}H-NMR and ^{13}C-NMR analysis. The ^{1}H-NMR is reported in Figure 6, and the signal assignments are following detailed.

BOA

^{1}H NMR (400 MHz, $CDCl_3$) δ 4.49 (d, J = 6.0 Hz, 2H), 4.37 (d, J = 5.9 Hz, 2H), 4.15 (s, 2H), 2.38 (t, J = 2.3 Hz, 2H), 1.76 – 1.60 (m, 2H), 1.32 (s, 3H).

^{13}C NMR (101 MHz, $CDCl_3$) δ 173.28, 79.55, 68.61, 39.08, 33.75, 24.36, 21.18.

BOI

^{1}H NMR (400 MHz, $CDCl_3$) δ 6.38 (s, 1H), 5.76 (s, 1H), 4.51 (dd, J = 13.4, 6.0 Hz, 4H), 4.38 (dd, J = 10.9, 6.0 Hz, 4H), 4.24 (s, 2H), 4.18 (s, 2H), 3.41 (s, 2H), 1.34 (s, 3H), 1.32 (s, 3H).

^{13}C NMR (101 MHz, $CDCl_3$) δ 170.57, 165.98, 133.46, 129.02, 79.42, 69.14, 69.09, 39.18, 39.09, 37.65, 21.15, 21.11.

TOC

^{1}H NMR (400 MHz, $CDCl_3$) δ 4.53 – 4.44 (m, 4H), 4.40-4.34 (m, 8H), 4.31 – 4.21 (m, 2H), 4.17 (s, 4H), 4.19 – 4.07 (m, 1H), 4.00 (s, 1H), 3.01 – 2.79 (m, 4H), 1.32 (s, 3H), 1.28 (s, 6H).

^{13}C NMR (101 MHz, $CDCl_3$) δ 173.29, 169.64, 79.40, 79.36, 79.27, 73.29, 70.19, 69.18, 69.11, 43.47, 43.39, 39.11, 39.05, 21.04.

4.3 | Formulation Preparation and Photopolymerization

The formulations were prepared by adding 6 phr (per hundred resin) of triarylsulfonium hexafluoroantimonate salts (S-SbF) as the photoinitiator (PI) to the synthesized monomers (BOA, BOI, and TOC), followed by mixing. The samples were then placed in a silicon mould and preheated in the oven at the mentioned temperatures (85°C, 105°C) and cured using DYMAX ECE Flood lamp (Dymax Europe GmbH) at a light intensity of 130 mW/cm^2. The curing duration ranged from 3 to 12 min, depending on the monomer's induction time.

4.4 | Characterization Methods

4.4.1 | Nuclear Magnetic Resonance (NMR) Spectroscopy

Chemical structures of the synthesized monomers were investigated by ^{1}H NMR spectroscopy performed on an Avance 400 (Bruker) spectrometer (400 MHz). CDCl3-d1 was used as the solvent and also as the internal standard for calibrating the chemical shift.

4.4.2 | Fourier Transform Infrared (FTIR) Spectroscopy

The structural changes of the oxetane monomers before and after UV-irradiation were evaluated by a PerkinElmer Spectrum 100 instrument (PerkinElmer Waltham, Massachusetts, US), in transmission mode. The FTIR spectra were acquired with a resolution of 4 cm^{-1} and obtained as the average of 32 scans. The liquid formulation was spread on a silicon wafer window by a film bar to obtain a thickness of 12 µm. The sample was exposed to UV light using a Hamamatsu LC8 mercury lamp with an 8 mm light guide and spectral distribution range of 240–400 nm with a light intensity around 130 mW/cm^2. The real-time FTIR (RT-FTIR) spectra were collected in the range of 4000–400 cm^{-1}. The degree of conversion was calculated using Equation (1), by monitoring the disappearance over time of the characteristic peaks at 835 and 980 cm^{-1} associated with the oxetane group [28, 45–51]. All measurements were conducted in triplicate.

$$Conversion\ (\%) = \frac{\left(\frac{A_{group}}{A_{ref}}\right)_{t=0} - \left(\frac{A_{group}}{A_{ref}}\right)_{t}}{\left(\frac{A_{group}}{A_{ref}}\right)_{t=0}} \times 100 \quad (1)$$

4.4.3 | Photo Differential Scanning Calorimetry (Photo-DSC)

To investigate the photo-crosslinking process, photo-DSC measurements were performed by using a Mettler Toledo DSC^{-1} instrument equipped with Gas Controller GC100 (Mettler Toledo Columbus, Ohio, US). A mercury lamp (Hamamatsu LightningcureTM LC8, Hamamatsu Photonics) with an optical fiber to directly irradiate the sample with a UV light emission centred at 365 nm and intensity at 100% was used. About 5–10 mg of the UV-curable liquid formulation was poured into an open 40 µL aluminium pan. An empty pan was used as a reference. The experiments were conducted at 25°C, 85°C, and 105°C under N_2 atmosphere with a flow rate of 40 mL min^{-1}. The heating method was performed with a rate of 10 K min^{-1}. The samples were subjected to UV irradiation twice for 10–15 min. The second UV light exposure step was required to confirm the complete UV curing and establish the baseline. The curing curve resulted from subtracting the second curve from the first. All tests were carried out in triplicate, and the data were elaborated by Mettler STARe software V9.2.

4.4.4 | Gel Content

The percentage of gel content (%) in the UV-cured samples was measured by placing approximately 300 mg of the UV-cured film for the extraction of the non-cured part in chloroform for 24 h at room temperature. After extraction, the samples were left to dry in air for 24 h. The gel content was then calculated using Equation (2):

$$\%gel = \frac{W_1}{W_0} \times 100 \quad (2)$$

where W1 represents the weight of the dried film post-chloroform treatment, and W0 is the initial weight of the sample.

4.4.5 | Dynamic-Mechanical Thermal Analysis (DMTA)

DMTA analysis of the thermosets was conducted using the TT-DMA instrument from Triton Technology LTd. Rectangular samples (0.5 mm×5 mm×25 mm) were prepared by photocuring of the formulations in silicon moulds, using DYMAX ECE Flood

lamp (Dymax Europe GmbH) at a light intensity of 130 mW/cm^2 for 3–12 min. The analysis involved a temperature ramp from −50°C to 110°C at a rate of 3°C/min, with uniaxial tensile stress applied at a frequency of 1 Hz. The glass transition temperature (Tg) of the materials was established as the peak of the tan δ curve.

The cross-link density (νc) per unit volume was calculated using Equation (3), which was derived from the statistical theory of rubber elasticity:

$$\nu_c = \frac{E'}{3RT} \tag{3}$$

where: νc is the number of crosslinks per volume of the crosslinked network, E' is the storage modulus at the rubbery plateau (Tg + 50°C), R is the gas constant, and T is the temperature expressed in Kelvin.

4.4.6 | Contact Angle

The contact angle on the UV-cured samples was measured on the free surface with bi-distilled water. The Drop Shape Analyzer DSA100 (Krüss) instrument was used. Five measurements were taken to have an average value.

Acknowledgements

This paper is part of a project that has received funding from the European Union's Horizon 2020 research and innovation program under the Marie Skłodowska-Curie grant agreement, No.101085759 (SURE-Poly).

Open access publishing facilitated by Politecnico di Torino, as part of the Wiley - CRUI-CARE agreement.

Conflicts of Interest

The authors declare no conflicts of interest.

Data Availability Statement

The data that support the findings of this study are available from the corresponding author upon reasonable request.

References

1. S. Caillol, B. Boutevin, and R. Auvergne, "Eugenol, a Developing Asset in Biobased Epoxy Resins," *Polymer* 223 (2021): 123663.

2. A. Richel, P. Maireles-Torres, and C. Len, "Recent Advances in Continuous Reduction of Furfural to Added Value Chemicals," *Current Opinion in Green and Sustainable Chemistry* 37 (2022): 100655.

3. E. Cousin, K. Namhaed, Y. Pérès, et al., "Towards Efficient and Greener Processes for Furfural Production from Biomass: a Review of the Recent Trends," *Science of The Total Environment* 847 (2022): 157599.

4. S. Raza, J. Zhang, I. Ali, X. Li, and C. Liu, "Recent Trends in the Development of Biomass-Based Polymers from Renewable Resources and Their Environmental Applications," *Journal of the Taiwan Institute of Chemical Engineers* 115 (2020): 293–303.

5. P. Chavan, A. K. Singh, and G. Kaur, "Recent Progress in the Utilization of Industrial Waste and by-Products of Citrus Fruits: a Review," *Journal of Food Process Engineering* 41 (2018): 12895.

6. A. Gandini, "Furans as Offspring of Sugars and Polysaccharides and Progenitors of a family of Remarkable Polymers: A Review of Recent Progress," *Polymer Chemistry* 1 (2010): 245–251.

7. E. Ramon, C. Sguazzo, and P. M. G. P. Moreira, "A Review of Recent Research on Bio-Based Epoxy Systems for Engineering Applications and Potentialities in the Aviation Sector," *Aerospace* 5 (2018): 110.

8. H. Nakajima, P. Dijkstra, and K. Loos, "The Recent Developments in Biobased Polymers toward General and Engineering Applications: Polymers That Are Upgraded from Biodegradable Polymers, Analogous to Petroleum-Derived Polymers, and Newly Developed," *Polymers (Basel)* 9 (2017): 523.

9. R. Auvergne, S. Caillol, G. David, B. Boutevin, and J.-P. Pascault, "Biobased Thermosetting Epoxy: Present and Future," *Chemical Reviews* 114 (2014): 1082–1115.

10. G. Mashouf Roudsari, A. K. Mohanty, and M. Misra, "Green Approaches To Engineer Tough Biobased Epoxies: a Review," *ACS Sustainable Chemistry & Engineering* 5 (2017): 9528–9541.

11. R. Luque, "Catalytic Chemical Processes for Biomass Conversion: Prospects for Future Biorefineries," *Pure and Applied Chemistry* 86 (2014): 843–857.

12. L. Pezzana, G. Melilli, P. Delliere, et al., "Thiol-ene Biobased Networks: Furan Allyl Derivatives for Green Coating Applications," *Progress in Organic Coatings* 173 (2022): 107203.

13. P. Sudarsanam, R. Zhong, S. Van Den Bosch, S. M. Coman, V. I. Parvulescu, and B. F. Sels, "Functionalised Heterogeneous Catalysts for Sustainable Biomass Valorisation," *Chemical Society Reviews* 47 (2018): 8349–8402.

14. H. Lai, J. Zhang, and P. Xiao, "Renewable Photopolymers: Transformation of Biomass Resources into Value-Added Products under Light," *ACS Sustainable Chemistry & Engineering* 11 (2023): 16365–16406.

15. M. Sangermano, N. Razza, and J. V. Crivello, "Cationic UV-Curing: Technology and Applications," *Macromolecular Materials and Engineering* 299 (2014): 775–793.

16. M. Sangermano, "Advances in Cationic Photopolymerization," *Pure and Applied Chemistry* 84 (2012): 2089–2101.

17. J. V. Crivello and S. Liu, "Photoinitiated Cationic Polymerization of Epoxy Alcohol Monomers," *Journal of Polymer Science A Polymer Chemistry* 38 (2000): 389–401.

18. L. Pezzana, G. Melilli, N. Guigo, N. Sbirrazzuoli, and M. Sangermano, "Cationic UV Curing of Bioderived Epoxy Furan-Based Coatings: Tailoring the Final Properties by in Situ Formation of Hybrid Network and Addition of Monofunctional Monomer," *ACS Sustainable Chemistry & Engineering* 9 (2021): 17403–17412.

19. M. Sangermano, "UV Cured Nanostructured Epoxy Coatings" in *Epoxy Polymers New Materials and Innovations*, eds. J. P. Pascault and R. J. J. Williams (Wiley, Weinheim: 2010): 235–251.

20. A. S. Pell and G. Pilcher, "Measurements of Heats of Combustion by Flame Calorimetry. Part 3.—Ethylene Oxide, Trimethylene Oxide, Tetrahydrofuran and Tetrahydropy," *Transactions of the Faraday Society* 61 (1965): 71–77.

21. Y. Yamashita, T. Tsuda, M. Okada, and S. Iwatsuki, "Correlation of Cationic Copolymerization Parameters of Cyclic Ethers, Formals, and Esters," *Journal of Polymer Science A1* 4 (1966): 2121–2135.

22. H. Sasaki and J. V. Crivello, "The Synthesis, Characterization, and Photoinitiated Cationic Polymerizaton of Difunctional Oxetanes," *Journal of Macromolecular Science, Part A* 29 (1992): 915–930.

23. J. V. Crivello and H. Sasaki, "Synthesis and Photopolymerization of Silicon-Containing Multifunctional Oxetane Monomers," *Journal of Macromolecular Science, Part A* 30 (1993): 173–187.

24. J. V. Crivello and H. Sasaki, "Structure and Reactivity Relationships in the Photoinitiated Cationic Polymerization of Oxetane Monomers," *Journal of Macromolecular Science, Part A* 30 (1993): 189–206.

25. U. Bulut and J. V. Crivello, "Reactivity of Oxetane Monomers in Photoinitiated Cationic Polymerization," *Journal of Polymer Science A Polymer Chemistry* 43 (2005): 3205–3220.

26. J. V. Crivello, ""Kick-Starting" Oxetane Photopolymerizations," *Journal of Polymer Science A Polymer Chemistry* 52 (2014): 2934–2946.

27. M. Sangermano, R. Bongiovanni, G. Malucelli, et al., "Synthesis and Cationic Photopolymerization of a New Fluorinated Oxetane Monomer," *Polymer* 45 (2004): 2133–2139.

28. M. Sangermano, G. Malucelli, A. Priola, and M. Manea, "Synthesis and Characterization of Acrylate–oxetane Interpenetrating Polymer Networks through a Thermal-UV Dual Cure Process," *Progress in Organic Coatings* 55 (2006): 225–230.

29. M. Sangermano, S. Giannelli, R. A. Ortiz, M. L. B. Duarte, A. K. R. Gonzalez, and A. E. G. Valdez, "Synthesis of an Oxetane-Functionalized Hemispiroorthocarbonate Used as a Low-Shrinkage Additive in the Cationic Ultraviolet Curing of Oxetane Monomers," *Journal of Applied Polymer Science* 112 (2009): 1780–1787.

30. K. Zheng, X. Zhu, X. Qian, J. Li, J. Yang, and J. Nie, "Cationic Photopolymerization of 3-Benzyloxymethyl-3-Ethyl-Oxetane," *Polymer International* 65 (2016): 1486–1492.

31. A. N. Joshi, "Agricultural Biomass to Adipic Acid–An Industrially Important Chemical," *European Journal of Sustainable Development Research* 6 (2022): m0184.

32. M. Lang and H. Li, "Sustainable Routes for the Synthesis of Renewable Adipic Acid from Biomass Derivatives," *Chemsuschem* 15 (2022): 202101531.

33. W. Deng, L. Yan, B. Wang, et al., "Efficient Catalysts for the Green Synthesis of Adipic Acid from Biomass," *Angewandte Chemie—International Edition* 60 (2021): 4712–4719.

34. D. R. Vardon, M. A. Franden, C. W. Johnson, et al., "Adipic Acid Production from Lignin," *Energy & Environmental Science* 8 (2015): 617–628.

35. M. Zhao, X. Lu, H. Zong, J. Li, and B. Zhuge, "Itaconic Acid Production in Microorganisms," *Biotechnology Letters* 40 (2018): 455–464.

36. H. Hajian and W. M. W. Yusoff, "Itaconic Acid Production by Microorganisms: a Review," *Current Research Journal of Biological Sciences* 7 (2015): 37–42.

37. T. Robert and S. Friebel, "Itaconic Acid—A Versatile Building Block for Renewable Polyesters with Enhanced Functionality," *Green Chemistry* 18 (2016): 2922–2934.

38. M. G. Steiger, M. L. Blumhoff, D. Mattanovich, and M. Sauer, "Biochemistry of Microbial Itaconic Acid Production," *Frontiers in Microbiology* 4 (2013): 23.

39. T. Cordes, A. Michelucci, and K. Hiller, "Itaconic Acid: The Surprising Role of an Industrial Compound as a Mammalian Antimicrobial Metabolite," *Annual Review of Nutrition* 35 (2015): 451–473.

40. A. R. Angumeenal and D. Venkappayya, "An Overview of Citric Acid Production," *LWT-Food Science and Technology* 50 (2013): 367–370.

41. J. V. Crivello, "Investigation of the Photoactivated Frontal Polymerization of Oxetanes Using Optical Pyrometry," *Polymer* 46 (2005): 12109–12117.

42. P. Kubisa, "Hyperbranched Polyethers by Ring-Opening Polymerization: Contribution of Activated Monomer Mechanism," *Journal of Polymer Science A Polymer Chemistry* 41 (2003): 457–468.

43. S. Penczek, J. Pretula, and S. Slomkowski, "Ring-opening Polymerization," *Chemistry Teacher International* 3 (2021): 33–57.

44. N. Guy, O. Giani, S. Blanquer, J. Pinaud, and J. J. Robin *Progress in Organic Coatings* 153 (2021): 106159.

45. F. Li, X. Guo, Y. Wang, and M. Jin *European Polymer Journal* 192 (2023): 112074.

46. J. V. Crivello and U. Bulut, "Photoactivated Cationic Ring-opening Frontal Polymerizations of Oxetanes," *Designed monomers and polymers* 8 (2005): 517–531.

47. J. N. Sivakami, L. Iordanov, C. Bae, and C. Y. Ryu, "Kick-Started Oxetanes in Photoinitiated Cationic Polymerization: Scale-up Synthesis and Structure-Property Studies," in *Proceedings of RadTech International UV & EB Technology Expo & Conference* (Chicago, 2016).

48. S. Park, L. J. Kilgallon, Z. Yang, D. Y. Ryu, and C. Y. Ryu, "Molecular Origin of the Induction Period in Photoinitiated Cationic Polymerization of Epoxies and Oxetanes," *Macromolecules* 52 (2019): 1158–1165.

49. M. Motoi, Nagahara, Yokoyama, et al. *The Chemical Society of Japan* 62 (1989): 180–184.

50. A. Ueyama, M. Mizuno, S. Kanoh, and M. Motoi, "Preparation of Polyoxetane Resins Having Polyoxirane Segments in the Pendant and Cross-Linking Chains and Uses as Polymeric Solvents for Alkali-Metal Ions," *Polymer Journal* 34 (2002): 944–953.

51. S.-Q. Fang, Y.-L. Pang, and Y.-Q. Zou, "Synthesis, UV-Curing Behavior and Surface Properties of New Fluorine-Containing Aromatic Oxetane Monomers," *Chinese Journal of Polymer Science (English Edition)* 36 (2018): 521–527.